Collisional vertical f -asymmetry effect

P Maget, J Frank, P Manas, R Dumont, T Nicolas, J-F Artaud, C Bourdelle, L Colas, M Goniche, O Agullo, et al.

Collisional transport and poloidal asymmetry distribution of impurities in tokamak plasmas, with application to WEST

P. Maget[1], J. Frank[1,2], P. Manas[1], R. Dumont[1], T. Nicolas[3], J-F. Artaud[1], C. Bourdelle[1], L. Colas[1], M. Goniche[1], O. Agullo[2], X. Garbet[1] , H. Lütjens[3] and the WEST team[#]

[1] CEA, IRFM, F-13108 Saint Paul-lez-Durance, France.
[2] Aix-Marseille Université, CNRS, PIIM UMR 7345, 13397 Marseille Cedex 20, France.
[3] Centre de Physique Théorique, Ecole Polytechnique, CNRS, 91128 Palaiseau, France.
[#] see http://west.cea.fr/WESTteam

Summary

- **Heavy impurity transport is a key issue in metallic wall tokamaks**
  - **Collisional part can be dominant over turbulent one in the core [1]**
- **Derivation of a fast analytical model for collisional impurity transport**
  - **Self-consistent Poloidal asymmetry and radial flux**
  - **Applicable to rotating & ICR Heated plasmas [2]**
  - **Compared with XTOR [3,4] simulations, and with NEO [5]**
- **Investigation on a rare case of Tungsten accumulation on WEST**
  - **ICRH-driven asymmetry could be the main mechanism**

Analytical approach for collisional impurity transport

Neoclassical impurity transport

- With a poloidal distribution parametrized as $n_a/\langle n_a\rangle = 1+\delta\cos\theta+\Delta\sin\theta$ [1]:

$$\langle\Gamma_a^{neo}\cdot\nabla r\rangle \approx -\langle n_a\rangle \frac{D_{PS}^a}{R_0}\left[\left(1+\frac{\delta}{\epsilon}+\frac{\delta^2+\Delta^2}{4\epsilon^2}\right)\mathcal{G}+\frac{1}{2}\left(\frac{\delta}{\epsilon}+\frac{\delta^2+\Delta^2}{2\epsilon^2}\right)\mathcal{U} -\frac{\delta_M}{2\epsilon^2}\left(1-\frac{m_i}{m_a}\frac{e_a}{e_i}\right)\left(1+\frac{\delta}{2\epsilon}\right)\right]$$

- with $D_{PS}^a \equiv 2q^{*2}m_a\nu_a T_a/(e_a^2\langle B^2\rangle)$, $\varepsilon=r/R_0$, $C_0^a\sim1.5$ and $k_i\sim-1.17$ in the banana regime

$$G=\partial_r\ln p_a-\frac{e_a}{e_i}\frac{T_i}{T_a}\partial_r\ln p_i+C_0^a\frac{e_a}{e_i}\frac{T_i}{T_a}\partial_r\ln T_i \qquad U\approx-(C_0^a+k_i)\frac{e_a}{e_i}\frac{T_i}{T_a}\partial_r\ln T_i$$

$$\delta_M = 2\epsilon(m_a/m_i)(T_i/T_a)M_i^2$$

Poloidal asymmetry

- The poloidal asymmetry is given by the parallel force balance

$$\delta+\delta_\phi^a-\delta_M = -\mathcal{A}\left[\Delta\mathcal{G}+\Delta\mathcal{U}-\mathcal{R}\delta_M\epsilon\Delta\right]$$
$$\Delta+\Delta_\phi^a = \mathcal{A}\left[(2\epsilon+\delta)\mathcal{G}+\delta\mathcal{U}-2\mathcal{R}\delta_M\right]$$

$$\mathcal{A}=q^2\nu_a/(\epsilon\Omega_a) \qquad \mathcal{R}=\frac{1}{2\epsilon}\left(1-\frac{m_i}{m_a}\frac{e_a}{e_i}\right)$$

- With the electrostatic potential modelled as $e(\phi-\langle\phi\rangle)/T_e = \delta_\phi\cos\theta+\Delta_\phi\sin\theta$ and

$$\left(\delta_\phi^a,\ \Delta_\phi^a\right)=Z_a(T_e/T_a)\left(\delta_\phi,\ \Delta_\phi\right)$$

Self-consistent collisional impurity transport model

- Implemented in FACIT code (FAst Collisional Impurity Transport)
- Impurity flux & asymmetry are non-linear functions of the impurity gradient
- Collisional friction couples vertical & horizontal asymmetry: tilting w.r.t. the drive

The natural case (no rotation, no ϕ asymmetry)

Poloidal asymmetry parameters (δ, Δ) move on a circle as collisionality varies

- Pinch velocity is strongly reduced by poloidal asymmetry at high Z (flat n_a) [6] *(fig.1)*

Fig.1 : Radial impurity flow as a function of the impurity charge Z_a with & without selft-consistent poloidal asymmetry (left); corresponding asymmetry (right). The impurity profile is flat.

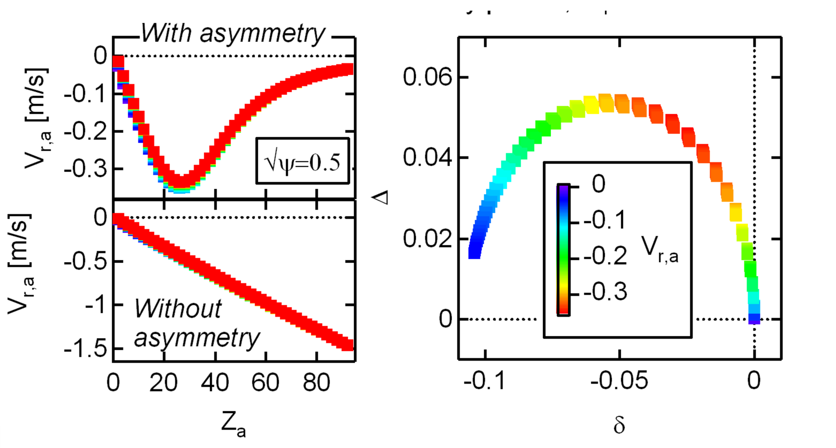

Numerical experiments with XTOR-2F code [2]

- Neoclassical physics [4]
- Impurity conservation and momentum equations
- The collisionality (ν_a) is scanned artificially
- The circle in the (δ, Δ) plane is recovered …
- … as well as the reduction of the pinch velocity *(fig. 2)*

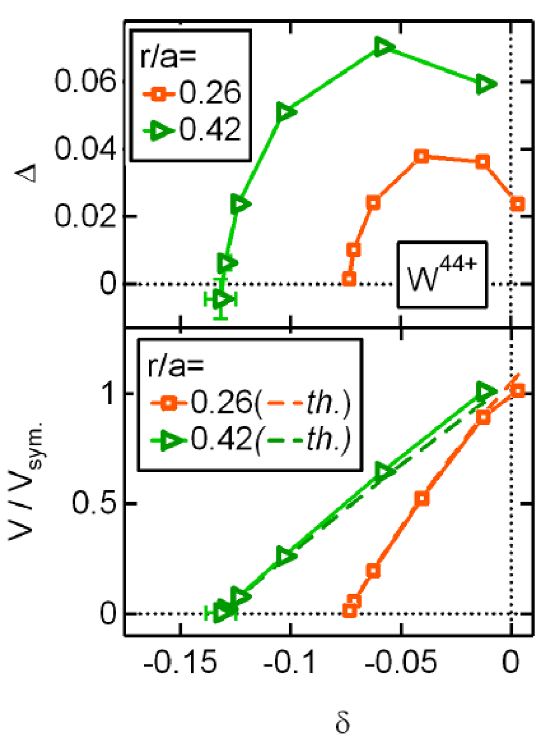

Fig.2 : Asymmetry (top) and ratio of radial flow to theoretical value without asymmetry (bottom): XTOR simulations & FACIT model

Neoclassical steady-state (Γ^{neo}=0)

- Poloidal asymmetry cancels *(fig. 3)*
- XTOR simulation follow same initial trajectory in (δ, Δ)

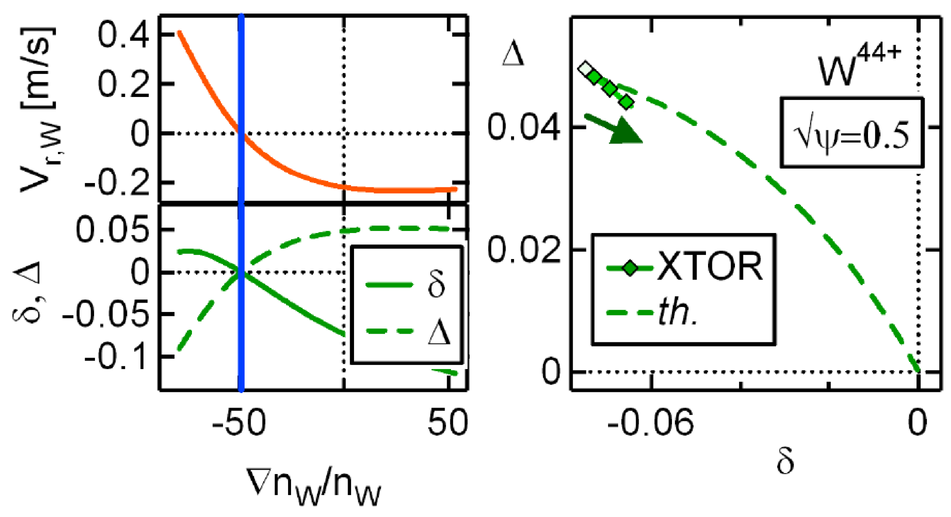

Fig.3 : Left: radial flux (top) and asymmetry (bottom). Right : XTOR simulations & FACIT model

Collisional vertical ϕ - asymmetry effect

Extension of the natural case to finite ϕ - asymmetry

- Ion-electron collisions drive a vertical ϕ - asymmetry [7]
- $$\Delta_\phi^{nat}\approx\frac{C^{nat.}}{Z_i+T_e/T_i}\frac{q^2x}{\epsilon^{5/2}}\frac{\partial_x\ln T_i}{\tau_{ii}\Omega_i}$$ with $C^{nat}\approx-0.165$
- Asymmetry recovered with NEO at 1rst order : not used for computing impurity flux
- But in fact, it strongly impact impurity flux & poloidal asymmetry in the absence of other drives (no rotation & no ICRH) *(fig.4)*
- Only effective at low T_i

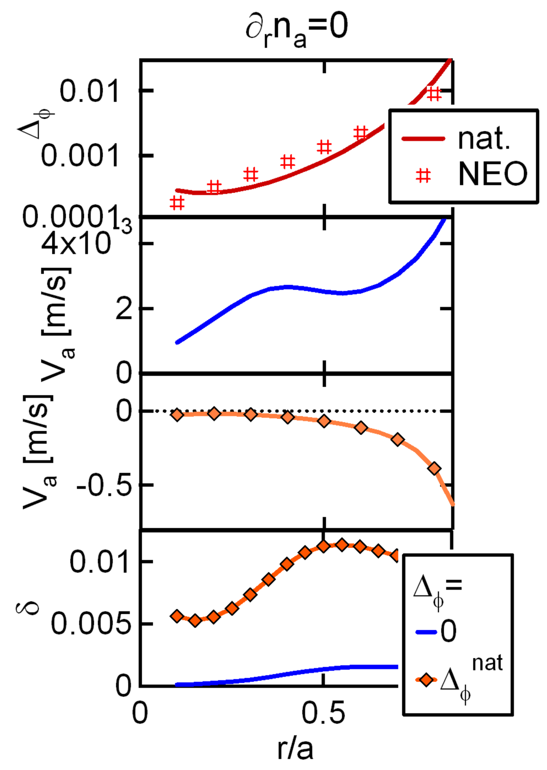

Fig.4 : Natural vertical electrostatic potential asymmetry profile, pinch velocity and horizontal asymmetry with and without Δ^{nat}, .

Toroidal rotation and ICRH effect

Toroidal rotation

- Neoclassical diffusion coefficient, pinch velocity and horizontal asymmetry at Γ^{neo}=0 in good agreement with NEO for M_i<0.3 *(fig. 5)*
- Pinch velocity overestimated above M_i<0.3
- Low Field Side localization due to centrifugal force

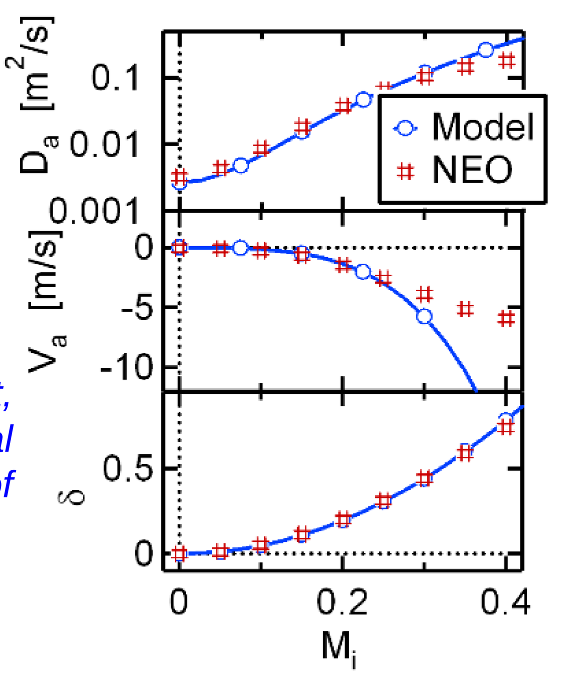

Fig.5 : Diffusion coefficient, pinch velocity and horizontal asymmetry as a function of the ion Mach number.

ICRH

- Minority temperature anisotropy : horizontal ϕ-asymmetry

$$\delta_\phi=\frac{\epsilon}{1+Z_iT_e/T_i}\left[f_H\left(\frac{T_\perp}{T_\parallel}-1\right)+m_i\frac{(R_0\Omega)^2}{T_i}\right]$$

- Neoclassical diffusion coefficient, pinch velocity and horizontal asymmetry at Γ^{neo}=0 agrees with NEO *(fig.6)*
- High Field Side localization due to electrostatic force
- Transition from expulsion to accumulation above a critical temperature anisotropy
- Neoclassical diffusion vanishes at the transition: classical diffusion dominant
- Favorable domain $T_\perp/T_\parallel < (T_\perp/T_\parallel)^{crit}$ expands with M_i as

$$\left[f_H\left(\frac{T_\perp}{T_\parallel}-1\right)\right]^{crit}\approx2\frac{Z_i+T_i/T_e}{Z_a}+2M_i^2\left[\frac{m_a}{m_i}\frac{Z_i+T_i/T_e}{Z_a}-1\right]$$

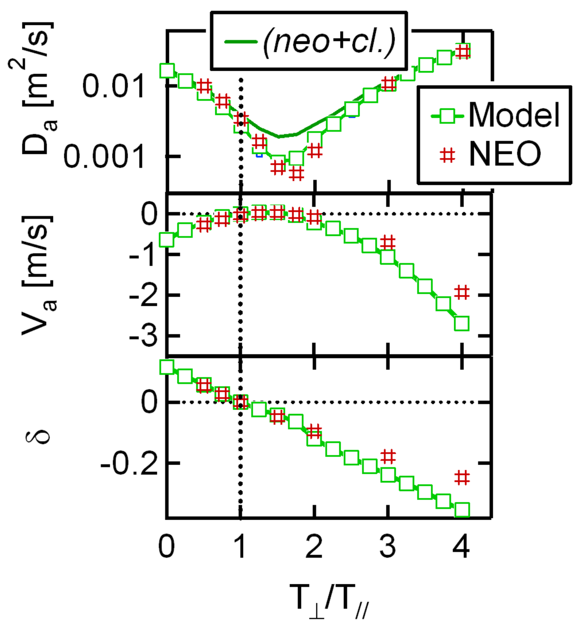

Fig.6 : Diffusion coefficient, pinch velocity and horizontal asymmetry as a function of $T_\perp/T_\parallel$.

Tungsten peaking & ICRH operation: a WEST case

Rare cases of Tungsten accumulation on WEST

- Low torque plasma: turbulent transport dominates [8]
- Accumulation observed in some ICRH pulses *(fig.7)*

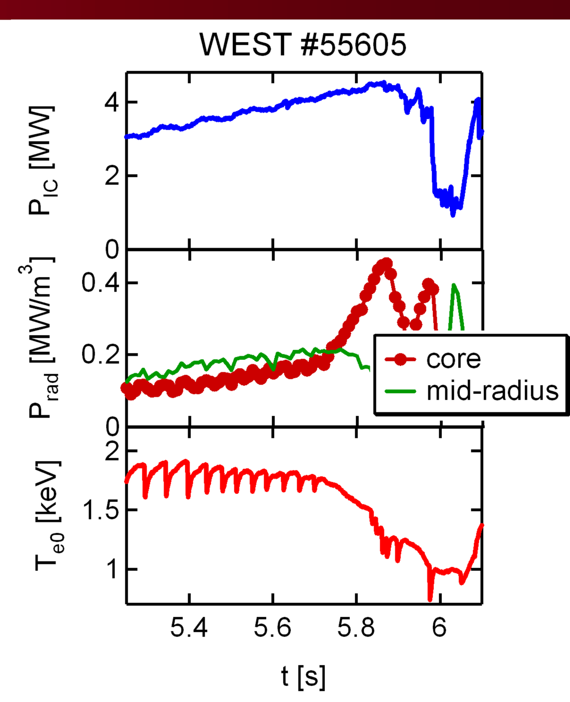

Fig.7 : ICRH power, radiative power and core electron temperature.

Modeling of Tungsten peaking

- Interpretative Integrated modeling with METIS [9]
- Ion temperature deduced neutron flux & $T_i\propto\sqrt{n_eT_e}$
- Minority temperature anisotropy : EVE/AQL [10] *(fig. 8)*
- Minority temperature screening effect not considered
- Toroidal rotation not measured but (1,1) MHD mode accelerates linearly with ICRH power *(fig.9)*
- Rotation: $V_\varphi=V_0+(V/P)\times P_{IC}$ with *(V/P)~3km/s/MW*
- Tungsten peaking from FACIT consistent with ICRH drive at low rotation *(V_0~0) (fig.10)*

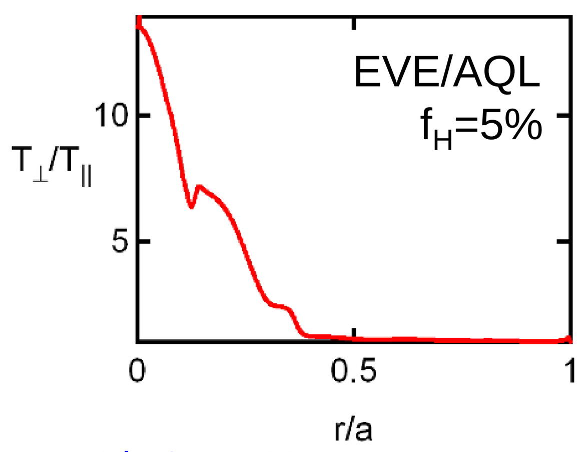

Fig.8 : H temperature anisotropy from EVE/AQL

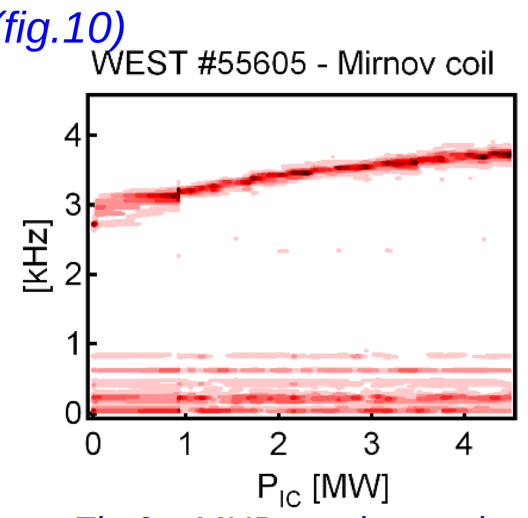

Fig.9 : MHD mode rotation as a function of P_{IC}.

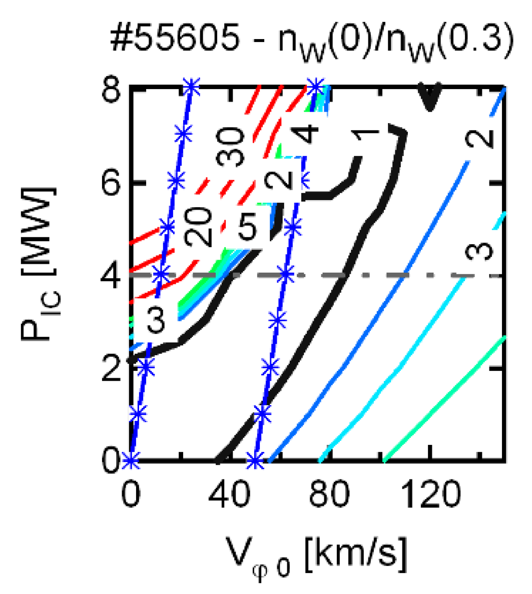

Fig.10 : Tungsten peaking in (P_{IC}, V_φ) map. Trajectories for V_0=0 and 50 km/s

References

[1] Angioni et al *PPCF* **56** 124001 (2014)
[2] Maget et al, *PPCF* **62** 105001 (2020)
[3] Lütjens *J. Comp. Phys.* **229** 8130 (2010)
[4] Maget et al, *PPCF* **62** 025001 (2020)
[5] Belli et al *PPCF* **50** 095010 (2008)
[6] Helander *Physics of Plasmas* **5** 3999 (1998)
[7] Hinton *The Physics of Fluids* **16** 836 (1973)
[8] Yang *Nuclear Fusion* **60** 086012 (2020)
[9] Artaud *Nuclear Fusion* **58** 105001 (2018)
[10] Dumont *NF* **49** 075033 (2009);*NF* **53** 013002 (2012)

Acknowledgements

This work has been carried out within the framework of the EUROfusion Consortium and the French Research Federation for Fusion Studies and has received funding from the Euratom research and training programme 2014-2018 and 2019-2020 under grant agreement No 633053 for the project ENR-MFE19.CEA-03. We benefited from HPC resources from GENCI (project 056348). The views and opinions expressed herein do not necessarily reflect those of the European Commission.